

Relationships between building damage and characteristics of strong ground motions during the M6.5 Zhaotong Earthquake-I

WANG, Xin^{1*} ; MA, Qiang² ; SI, Hongjun³ ; DANG, Ji⁴ ; WU, Hao⁵ ; KURAHASHI, Susumu⁶

¹IRIDeS, Tohoku University, ²Institute of Engineering Mechanics, China Earthquake Administration, ³Earthquake Research Institute, The University of Tokyo, ⁴Saitama University, ⁵DPREC, Aichi Institute of Technology, ⁶Aichi Institute of Technology

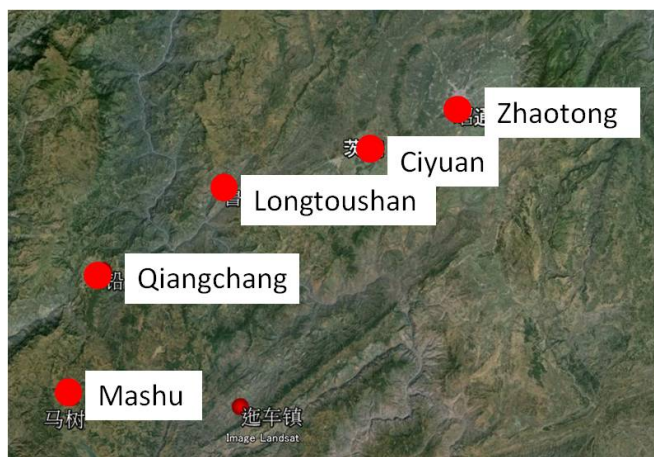
Magnitude 6.5 inland earthquake happened at the Longtoushan town which is located on the northeast side of the Yunnan province of China on 16:30 August 3rd, 2014 (CST). The biggest seismic intensity is estimated to be IX in China seismic intensity scale (equal to 5+ in JMA seismic intensity scale) at the Longtoushan town with the recorded peak ground acceleration (PGA) of 949 gal. As of 8 August 2014, 617 persons were killed by this earthquake, in which almost 85% (526 persons) of the death are happened at the Longtoushan town. The reason of death should be attributed to the seismic capability of residential houses and the characteristics of ground strong motions.

In order to make clear the building damage condition and the ground amplitude and period characteristics, we performed the onsite investigation of building damage and the microtremor measurement from November 9th ~12th, 2014. The places which have been investigated are marked with red dots in Fig 1. The PGA of investigated places are, 15 gal at Zhaotong city, 45 gal at Ciyuan town, 137 gal at Qianchang, and 135 gal at Mashu town. Based on the attenuation relations of PGA, it has been known that the accelerations attenuated fast with the increasing of fault shortest distance.

Masonry houses and buildings are commonly used in the disaster area. In the Longtoushan town, the collapse of masonry buildings can be widely seen. Based on the vulnerability functions of the 2008 Wenchuan earthquake, which was proposed by Wang 2011, the predicted collapse ratio of the Longtoushan town is 79%, which is almost the same with the result of onsite investigation. However, the building collapse cannot be seen in other places. Some slight damage, such as the crack in masonry walls, can be seen in the Qianchan town and Mashu town. Generally, no damage happened to buildings in the Zhaotong city.

We measured the ground microtremor of these onsite investigated places using high-sensitive velocity seismometers with sampling rate of 100 Hz and duration of 30 min in each place. Based on the H/V spectra, the predominant period of Longtoushan is about 4 Hz which is almost the same with results of other places. Furthermore, it has been known that the building damage in Longtoushan town relates to the ground condition of mountain side and the river side.

Keywords: Zhaotong Earthquake, Onsite Investigation, Ground Microtremor Measurement, Masonry Buildings



Relationships between building damage and characteristics of strong ground motions during the M6.5 Zhaotong Earthquake-2

KURAHASHI, Susumu^{1*} ; IRIKURA, Kojiro¹ ; WANG, Xin² ; SI, Hongjun³ ; MA, Qiang⁴ ; WU, Hao¹

¹Aichi Institute of Technology, ²IRIDeS, Tohoku University, ³Earthquake Research Institute, The University of Tokyo, ⁴Institute of Engineering Mechanics, China Earthquake Administration

On 3 August 2014, an Ms6.5 earthquake occurred at the Longtoushan town located on the northeast side of the Yunnan province of China. As of 8 August 2014, 617 persons were killed by this earthquake, in which almost 85% (526 persons) of the death happened in the Longtoushan town. During this earthquake, the strongest peak acceleration of 949 gal was measured in the Longtoushan station (LLT station). The observed record at the station also had two impulsive waves (figure (b)). Explication of generation mechanism of the large acceleration is needed to clear the relationship between seismic ground motion and damage. In this study, we construct the strong motion generation area (SMGA) as the short-period source model of this earthquake using the strong-motion records, and elucidate generation mechanism of the large acceleration.

The aftershock distribution of this earthquake is shown in Figure (a). Two possible fault planes from the distribution are considered to be southeast ? northwest (plane A) and southwest ? northeast (plane B).

Most of building damage and landslide disasters were along the plane A. On the other hands, although the slip distribution on each plane was inverted by the teleseismic data, we do not understand which plane is better from the results.

Therefore, we try to estimate the short-period source model using the empirical Green's function method. In the first trial, we did not use the LLT station's data too close to the source fault because the rupture plane is not clear. The earthquake information about the hypocenter of the mainshock and aftershocks is not enough to determine the rupture planes correctly. Therefore, the seismic moment of the element event used as the empirical Green's function is calculated from magnitude, and the seismic mechanism of the element event is assumed to be the same as the mainshock. The scaling parameters N and C are determined for SMGA from the observed source spectral ratio between the mainshock and the element event.

The synthetic ground motions explain well the characteristics of observed ground motions for either plane. The area and stress drop of the SMGA were about 100km² and about 10 MPa, respectively. However, we do not understand which plane is better.

Next, we discussed the arrival direction of seismic waves by the particle motion diagrams of the two impulsive waves using the observed record at LLT station.

The NS and EW particle motion of P-waves in the horizontal plane oscillate in northwest-southeast direction. Namely, the azimuth of the starting point of fault rupture is assumed to be northwest direction (Fig(c) left figure).

Similarly, the particle motion diagrams of the first pulse and second pulse of S-wave oscillate in northwest-southeast and northeast-southwest direction, respectively. If these pulses mainly consist of SH wave, the propagation directions from those two pulses seem to be different. As a result, the first and second pulses are assumed to be generated from plane A and plane B, respectively to satisfy the relation between the aftershock distribution and the location of observation station (LLT).

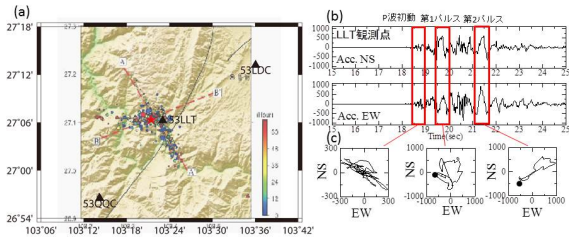
Hereafter, we try to estimate the strong-motion generation areas using LLT station's record.

Keywords: Zhaotong Earthquake, large acceleration, strong-motion generation area

SSS25-02

Room:A04

Time:May 25 09:15-09:30



Relationships between building damage and strong ground motions characteristics during the 2014 Zhaotong Earthquake-III

WU, Hao^{1*} ; WANG, Xin² ; SI, Hongjun³ ; DANG, Ji⁴ ; MA, Qiang⁵ ; LIN, Guoliang⁶ ; IRIKURA, Kojiro¹ ; KURAHASHI, Susumu¹

¹Aichi Institute of Technology, ²Tohoku University, ³The University of Tokyo, ⁴Saitama University, ⁵China Earthquake Administration, IEM, ⁶Yunnan Province Earthquake Administration

Many of the buildings near the Longtoushan (LTS) strong-motion station were heavily damaged or collapsed during the 2014 Zhaotong earthquake (Ms 6.5) which occurred on Aug. 3, 2014. The largest PGA with approximately 1 g was recorded at LTS during the mainshock. In contrast, the damage of buildings was minor near other stations, and the strong-motion records there were lower than 150 gal.

We conducted an almost three-day field survey near five strong-motion stations around the epicenter. We found that the causes for heavy damage of buildings near the LTS station were complicated, such as geological failure (e.g. landslide), insufficiently seismic resistant structural design, inappropriate construction, and site effect (transfer function and nonlinear effect), and so on. We also found that the collapse of many buildings in the EW direction was obviously heavier than that in the NS direction near the LTS station. It can be explained by the higher pseudo-velocity response spectrum in the range of 0.5 s to 1.0 s in the EW direction.

We also conducted microtremor measurement at six sites around the LTS station to examine the variation of site effects in this area. We found that the predominant periods at heavily damaged sites were similar, i.e., 0.25 s, while the predominant periods at light damaged sites were about 0.15 s.

In addition, we obtained several aftershock records as well as mainshock record, and the boring data near the LTS station. These data can be used to clarify the site effect characteristic at the LTS station.

Keywords: Zhaotong Earthquake, ground motion, microtremor, site effect

STRONG GROUND MOTION SIMULATION of THE 24 MAY 2014 NORTH AEGEAN SEA EARTHQUAKE (Mw 6.9) in TEKIRDAG and SURROUNDING AREA

KARAGOZ, Ozlem^{1*} ; CHIMOTO, Kosuke¹ ; YAMANAKA, Hiroaki¹ ; OZEL, Oguz³ ; CITAK, Seckin ozgur⁴

¹Department of Environmental Science and Technology, Tokyo Institute of Technology, Tokyo, Japan, ²Department of Geophysical Engineering, Canakkale Onsekiz Mart University, Canakkale, Turkey, ³Department of Geophysical Engineering, Istanbul University, Istanbul, Turkey, ⁴JAMSTEC

The Marmara Region (NW Turkey) was affected from destructive earthquakes since historical times. The North Anatolian Fault with 1,200 km length is the main source of the earthquakes in the region. The most recent 1999 Kocaeli Earthquake (Mw 7.4) damaged residential and industrial areas of the large cities in Marmara. The future earthquake is expected on the north-western segment of the fault close to the city of Tekirdag.

In this study, we simulated strong ground motion records of the 24 May 2014 North Aegean Sea Earthquake (Mw 6.9) in Tekirdag and surrounding area. We used one-dimensional homogeneous horizontal layer model at each AFAD (Republic of Turkey Prime Ministry Disaster & Emergency Management Presidency Earthquake Department) strong motion station site in Tekirdag and surrounding area (i.e. 5904, 5902, 5907, 5906), Canakkale (i.e. 1701, 1710), Gokceada (1711), Edirne-Enez (2201). We combined our shallow model (0-250 m) that obtained from our previous microtremor explorations (Karagoz et al., 2014) and the deeper parts were taken from previous crustal studies in the region. The outer fault parameters of the mainshock (seismic moment, strike, dip, and rake) were determined by previous focal mechanism solutions studies while the inner fault parameters were estimated by following the recipe of Irikura and Miyake (2011).

The fault plane (background) and asperities were divided into several subfaults that were assumed as single double-couple point source. We defined appropriate Kostrov-like slip-velocity function (modified by Nakamura and Miyake, 2000) for the asperity areas to simulate high frequency ground motions. The synthetic seismograms were obtained using a deterministic discrete wave number method for each sub-fault and were summed to get full waveform at the station around the epicentre in a broadband frequency range (0.1-10Hz).

The simulated peak ground velocities at the ground surface were estimated by multiplying the simulated ground motion at the top layer of $V_s=780$ m/s from the discrete wave number method with 1D amplification factors of S-waves in the shallow soil layers derived from the microtremor explorations. For validation, the results converted accelerations and were compared with S-wave portions of the recorded acceleration waveforms at the strong motion stations.

Keywords: Discrete wave form method, earthquake waveform simulation, Gokceada, site effect, Tekirdag

Source Rupture Process of the 2014 Northern Nagano Earthquake Estimated by Strong Motion Data

ASANO, Kimiyuki^{1*}; IWATA, Tomotaka¹; KUBO, Hisahiko¹

¹Disaster Prevention Research Institute, Kyoto University

A large inland crustal earthquake occurred in the northern Nagano prefecture, central Japan, on November 22, 2014 (M_{JMA} 6.7). According to the moment tensor solutions by Global CMT Project and F-net (NIED), this earthquake was a reverse-slip type event. This event has been reported to be related to an active fault, the Kamishiro fault of the Itoigawa-Shizuoka Tectonic Line (e.g., HERP, 2014). The surface rupture is observed along the Kamishiro fault. We estimated the source rupture process of this earthquake by the kinematic waveform inversion analysis using strong motion data.

We used strong motion data from 12 strong motion stations of K-NET, KiK-net, JMA, and Nagano prefecture. The S-wave portion of the velocity waveform in 0.05-1 Hz are used in the inversion analysis. Since the underground velocity structure in this region seems complex, it is not good strategy for calculating Green's functions that single one-dimensional velocity structure is applied to all stations. We assumed individual one-dimensional velocity structure model for each station, which is extracted from the nation-wide three-dimensional velocity structure model, Japan Integrated Velocity Structure Model Version 1 (JIVSM, Koketsu *et al.*, 2012). The Green's function was calculated by the discrete wavenumber method (Bouchon, 1981) and the reflection and transmission matrix method (Kennett and Kerry, 1979).

The fault model consists of two fault planes, which have different dip angle between the north and south plane based on the aftershock distribution by NIED (2014) and the surface fault information. The south fault plane has relatively steep dip angle compared to the north fault plane. The top of the south fault plane corresponds to the Kamishiro fault. The total length and width of the fault plane is 22 km and 14 km, relatively. The fault plane is divided into subfaults of 2 km \times 2 km. The moment function of each subfault is represented by a series of six smoothed ramp function.

The kinematic waveform inversion method is based on the multiple time-window linear waveform inversion method by Hartzell and Heaton (1983). The relative strength of the smoothing constraint (Sekiguchi *et al.*, 2000) and the first time-window front triggering velocity were determined to minimize Akaike's Bayesian Information Criteria.

The estimated source model has a large slip area in a slightly deep portion approximately 5 km north to the rupture starting point. Its largest slip is 1.8 m. It is consistent with the centroid location of the CMT solutions by GCMT and JMA. The aftershock activity in this large slip area is relatively low compared to the other area on the fault. The slip amount of the shallowest subfaults are approximately 0.3-0.5 m, and this slip would be related to the surface rupture observed after this earthquake. The total seismic moment is 3.85×10^{18} Nm (MW 6.3), and the average slip is approximately 0.4 m. Comparing these source parameters with previous inland crustal earthquakes in Japan, this earthquake is not an unusual earthquake.

Acknowledgments: The strong motion data of K-NET and KiK-net of NIED, JMA, and Nagano prefecture government which is released through SK-net of the Earthquake Research Institute, University of Tokyo, are used in this study.

Keywords: the 2014 northern Nagano earthquake, source process, strong motion data

Site amplification in Hakuba from microtremor and aftershock observation of the 2014 Northern Nagano Earthquake

CHIMOTO, Kosuke^{1*} ; YAMANAKA, Hiroaki¹ ; SAGUCHI, Koichiro¹ ; TSUNO, Seiji² ; MORIKAWA, Hitoshi¹ ; IIYAMA, Kahori¹ ; GOTO, Hiroyuki³

¹Tokyo Institute of Technology, ²Railway Technical Research Institute, ³DPRI

During the 2014 Northern Nagano Earthquake on 22 November, the maximum seismic intensity of 6 lower, buildings in Horinouchi or Mikkaichiba in Hakuba located at about 5km south to K-NET Hakuba were heavily damaged. We then carried out the aftershock observation and microtremor measurements from 24 November to 4 December to investigate the site amplification due to subsurface structure.

We carried out the aftershock observation with 13 temporal stations using accelerometer JEP6A3 with Data logger of LS7000XT and LS8800. We observed about 30 events with the seismic intensity of above 1, the highest peak ground motion was about 30 gal. In Horinouchi and Mikkaichiba, where the damage was heavy, we observed high accelerations and long later phases. The response spectrum shows high value between the periods of 0.5 and 1 second. The spectral ratios to the aftershock observed at the base of mountain in Mikkaichiba shows the peaks in the periods of 0.5 to 1 second.

We conducted microtremor measurements at all aftershock observation stations with the array size of less than 20m and applied SPAC method to estimate Rayleigh wave phase velocity. Near Horinouchi, we also conducted microtremore measurements with the large array size of about 680m at the west and east of Kamishiro Fault. We estimated dispersion curve of phase velocity in the range from about 3 to 30 Hz from the array size of about 20m. It was highest in K-NET Hakuba, and about 100 to 200m/s in Horinouchi and Mikkaichiba. We also estimated phase velocity of more than 1000m/s at above 1 second from large array. The S-wave velocity structures were estimated from an inversion of phase velocity. The layer with the S-wave velocity of 300m/s was less than 10m in K-NET Hakuba, while the layer with the S-wave velocity of below 200m/s was about 10m depth and about 50m thickness of the layer with 400m/s. The S-wave velocity structure obtained from the analysis of large arrays revealed that it was deeper in the west of the fault than the eastern part. The depths to the layer with the S-wave velocity of above 1000m/s were about 700m in the west and about 400m/s in the east. Since the depth to such layer in the KiK-net site, about 1km west to K-NET Hakuba, is below 100m, the heavily damaged area has deep structure in around the region.

We calculated the S-wave site amplification factor using the estimated S-wave velocity structure. The site amplification of shallow structure exhibits a peak at about 0.1 second in K-NET Hakuba, while it was about 1 second in Horinouchi and Mikkaichiba. The comparison between the spectral ratios and calculated site amplifications show similarity in terms of dominant periods. However, the spectral ratios have higher values in general, suggesting the effects of deep structures.

Keywords: 2014 Northern Nagano Earthquake, Site Amplification, Aftershock observation, Microtremors, Kamishiro Fault

Damages of Stone Lanterns at Zenkoji Temple, Nagano, Caused by Northeastern Nagano Earthquake, November 22, 2014

KATO, Mamoru^{1*}

¹GSHE, Kyoto University

Stone lanterns at Zenkoji Temple, Nagano, are severely damaged by the ground shaking caused by Northeastern Nagano Earthquake, November 22 2014. Damages of the residential houses in downtown Nagano is minor compared that in Hakuba Valley, and the damages at Zenkoji appear to be the result of characteristic ground shaking in downtown Nagano.

An M 6.7 earthquake occurred at the northern portion of Itoigawa-Shizuoka Tectonic Line on November 22, 2014. Seismic shaking in the vicinity of epicenter is as severe as JMA Intensity 6-minus, which caused moderate damages of the residential houses and geomorphology damages such as movement of surface ground mass.

Nagano Zenkoji Temple is located in downtown Nagano, approximately 30 km east of the epicenter. Strong shaking by this earthquake cause a number of stone lanterns at Zenkoji to collapse but the damages in the surrounding residential area is minor. Similar damages of stone lanterns are recorded at the previous large earthquake in this epicentral area in 1714. Collapse of stone lanterns often is interpreted as the strength of shaking is as strong as JMA Intensity 5 Reported Seismic Intensities are 5-plus and 4 at JMA Nagano and 4 at K-net, respectively..

We surveyed damages at Zenkoji Temple and investigate characteristics of strong motion in downtown Nagano. Our focus is on directions of collapse of stone lanterns which would be used to study direction of strong shaking. Our field surveys took place on November 23, the next day of the earthquake, and November 30 and December 1, one week later. Previously we have surveyed stone lanterns of Zenkoji Temple in 2013 to study whether these lanterns have recorded damages by 1847 Zenkoji Earthquake, and by using this result we are able to distinguish old and new damages of these lanterns.

Our results indicate that approximately one-thirds of the stone lanterns at Zenkoji Temple fell down by the strong shaking. Damages appear to occur in the entire Zenkoji area, and it is not successful to relate these damages to local site effects within Zenkoji. Stone lantern most frequently fell down toward south. Characteristic periods of typical stone lanterns are often assumed to be 0.2 or 0.5 second, and our results imply that shaking at high frequency is particularly strong in north-south direction at Zenkoji.

Keywords: String Motion, Northern Nagano Earthquake, 2014

Age-dependent Mortality in the 2011 East Japan Giant Earthquake (5) Additional Revision of the Current Equation

OHTA, Yutaka^{1*}; SHIGAKI, Tomoko²; KOYAMA, Maki³

¹Tono Res. Inst. Earthq. Science, ²Inst. Elderly Housing Sci., ³Medical Inst., Kyoto Univ.

1. Preface

This paper reports an additional revision for the current age-band specific mortality equation, though known as the traditional one, via critical examinations conducted in a series of previous studies. The current equation defined so as to describe Age-band specific mortality is effective enough to describe the deaths of elderlies, but lesser effective at evaluation of the deaths for infants and children, which suggests strongly the necessity of revision of the current equation.

What we attempted was to introduce two independent equations; one was made via slight revision of the Ozaki method commonly known in Medical Science and the other was made by developing a new equation based on an opinion by Sen in economics as earlier deaths such as either by starvation or poverty is nothing but the deprivation of all of capability. Those new equations brought better outcomes for the cases in the 2011 East Japan Earthquake. But, the first one revised starting from the Ozaki method was still insufficient for the direct comparison with the current mortality, since the first one produces a better figure for the absolute number of deaths but was not enough to produce mortality itself.

2. Additional Revision of the Ozaki method

In the revised equation of the Ozaki method, therefore, the values in the vertical axis were as just the number of deaths until the previous study and therefore no direct comparison with the currently known equation was incapable. In this paper we attempted additional revision by which the age-dependent mortality can directly be expressed and therefore a parallel comparison with current and traditional age-specific mortality equation is to be made. Our proposal at present is to introduce our newly revised mortality equation, having an equation composed under the proposal by Sen as a supporting equation.

3. Singularities in Mortality Curves among Prefectures and Municipalities

In comparison of such additionally revised equation and regarded curves with those smoothed ones, we are easy to recognize significant gaps between observed and smoothed ones, which suggest additional reasons over the main reason of the age-dependency due to the degeneration of behavioral performance of residents.

Here, we can point out a few singular cases; the most peculiar gap is seen at age-intervals of 0 up to 14, as has been known in a word called such as a Miracle in Kamaishi city in the curve of Iwate pref. Another remarkable gaps can be seen at 20-30 and 60-70 years old; for these unusual phenomena we have still been conducting the insight studies.

4. Concluding Remarks

We arrived at a conclusion that the age-dependent characteristics should be described in a manner different from the traditional and called current equation. And, in this way of thinking, we developed new equation sets which are more logical and effective at elucidating the mortality which may suffer in natural disasters as earthquakes and/or tsunamis. It is needless to say that the similar investigation is expected to be made for the other pattern than ones described

in the English J character types.

References

- 1) Ohta and Koyama; Mortality in the 2011 East Japan Earthquake (2, 3 and 4).
- 2) Katada; Hito ga shinanai bousai (Disaster Preparedness for Minimizing Death Toll, 2012, Shueisya Publishing Co., (in Japanese).
- 3) Ozaki; kousei no shihyou, 59, 2012 (in Japanese).
- 4) Amartya Sen, Retrieve via Wikipedia, giving his name as a serching string.

Keywords: East Japan Earthquake, Age-band specific Mortality, Revision of Evaluation Equation, Disaster-Vulnerable Persons

Multiple Seismic Origins of the 2011 Tohoku Earthquake Analyzed by S-Wave Peak and Regions

NUMAKURA, Masayuki^{1*}

¹Last position Sakura Higashi High School

1, Introduction

Within the field of research on the 2011 Tohoku earthquakes, analyses of the vicinity of the ocean trench axis have made remarkable progress. In contrast, opinion is divided regarding regions closer to land. One example concerns the question of whether tremors that reached the Kanto region originated from the ocean trench axis. Many studies emphasize land-based seismic origins for these tremors, but the precise locations from which these tremors originated remains to be determined in detail. Considering that this earthquake was a ones-in-several-hundred-years event, it can hardly be said that our understanding of the earthquake as a whole has progressed to a fully satisfactory state.

The S-wave and P-wave data available for this earthquake are mixed together and hence difficult to use. Multiple large-amplitude contributions following S-wave initial shocks, S-wave peaks, were present. These data may be used for analyses, despite their mixed nature, if they can be well separated. Due to the paucity of previous research on this subject, we have tested our methods on other large earthquakes in Japan. Method is indicated to 3-1-2 Results of validation.

2, Method

2-1 We determined epicenters by following the Omori method of drawing three circles on map.

2-2 We use Omori's formula. (However, we use distant-dependent velocities.)

$$r=k \times t \quad k1=(Vp \times Vs)/(Vp-Vs)$$

2-3 We used S-wave peak travel times and velocities. The method is indicated to 3-1-2.

3, Results

3.1 Validation.

3-1-2 2004 Niigata Chuetsu earthquake

Epicenter 37.29N 138.87E Depth 12km Start ; 17:56:00

Ojiya Distance 13.9km Traveltime S-wave peak 8.73s

Velocity peak 3.19km/s Acceleration 0.365 Constant 1.16 Time arrival 56:08

Tokamachi Distance 24.1km Travel time S-wave peak 12.60s

Velocity peak 3.83km/s Acceleration 0.304 Constant 1.16 Time arrival 56:12

Kashiwazaki Distance 31.0km Travel time S-wave peak 14.90s

Velocity peak 4.16km/s Acceleration 0.280 Constant 1.16 Time arrival 56:14

Travel time is peak time at many stations. (2) $r=1/2 \times a \times t^2$ (3) $r=1/2 \sqrt{kt^3}$

(4) $r=1/2 \times v \times t$ (5) $k=v \times a$ (6) $v=2r/t$ (7) $a=2r/t^2$ (8) $a=dv/dt$

It is sufficiently possible to calculate in this equation (2), but coefficient " a " is not constant. Therefore, I prepare the equation (3). The equations (2) and (3) are function that the distance and time of the hypocenter and observation point. In those equations, the function (5), which is in inverse proportion to " v " and " a ", is contained.

3-2 Seismic origins of 2011 Tohoku Earthquake

P-1-2 (Epicenter announced by United States Geological Survey)

Epicenter 37.291N 138.867N Depth 30km Start: 46minites, 24 seconds

Oshika Distance 81.5km Travel time S-wave peak 43.3s

Velocity peak 3.76km/s Acceleration 0.0868 Constant 0.327

Time arrival 47:07

Utatsu Distance 94.1km Travel time S-wave peak 47.6s

Velocity peak 3.95km/s Acceleration 0.0829 Constant 0.327

Time arrival 47:11

Tsukidate Distance 130.9km Travel time S-wave peak 59.3s

Velocity peak 4.41km/s Acceleration 0.0744 Constant 0.327

Time arrival 47:23

P-3, Epicenter 38.045N 141.47E Depth 30km Start: 47minites, 37 seconds

Oshika Distance 41.8km Travel time peak 20.0s

SSS25-09

Room:A04

Time:May 25 11:15-11:30

Velocity peak 4.18km/s Acceleration 0.209 Constant 0.873

Time arrival 47:57

Kamaishi Distance 143.6km Travel time peak 45.4s

Velocity peak 6.33km/s Acceleration 0.139 Constant 0.873

Time arrival 48:22

Hitachi Distance 180.2km Travel time peak 53.0s

Velocity peak 6.80km/s Acceleration 0.128 Constant 0.873

Time arrival 48:30

P5 (May be divided into 5 epicenters in all)

In the first phase, P1-2 and P1-3 gave a strong motion to Miyagi and Iwate. In the third phase, Max acceleration of Tsukidate and Oshika was observed by P3. It is both epicenter third phase and trench axis that gave a strong motion to Kanto.

Keywords: S-Wave Peak, 2011 Tohoku Warthquake

Simulation of strong ground motions from the Evaluation of the 2011 Mw 9.0 Tohoku earthquake

IRIKURA, Kojiro^{1*} ; KURAHASHI, Susumu¹

¹Aichi Institute of Technology, Disaster Prevention Research Center

The 2011 Mw 9.0 Tohoku earthquake occurring in the subduction zone off the Pacific coast of Tohoku, Japan was observed by dense networks of geophysical instruments including strong-motion, teleseismic, tsunami, and geodetic sensors. Long-period source models have been constructed from separate and joint inversions of long-period data including long-period strong motion data. On the other hand, short-period source models have been done from the back-projection method using short-period teleseismic data and the empirical Green's function method using strong motion data. Most of slip distribution inverted from long-period records such as geodetic and tsunami data are placed at depths shallower than the hypocenter toward the trench. On the other hand, short-period seismic energy obtained by the back-projection method was generated mainly from the down-dip areas near the coasts of Pacific coast. The observed strong motions have five wavepackets that correspond to specific strong-motion generation areas (SMGAs). The origins of the wavepackets were retrieved from the original seismograms using a semblance analysis. Then, we estimate a short-period source model for generating strong ground motions from this earthquake by comparing the observed records from the mainshock with synthesized motions based on a sperity/SMGA(strong motion generation area) source model and the empirical Green's function method. We find that five small-asperities in the down-dip areas generate short-period motions of engineering interest but large asperities in the shallower area east of hypocenter generate mainly long-period ground motions. We call such small asperity SMGA. Another problem is that the short-period source models with such SMGAs cannot simulate impulsive waves with high acceleration and velocity seen at onsets of the wave-packets in strong motion records observed near the source fault. To generate the impulsive waves, more heterogeneous model is needed with higher stress parameters within a small sub-area inside the SMGAs. Then we propose multi-scale heterogeneous model as a recipe of predicting strong ground motions for mega-thrust subduction earthquakes. Recent other Mw 9.0 class subduction earthquakes such as the 2004 Mw 9.1 Sumatra earthquake and the 2010 Mw 8.8 Maule earthquake are known to have almost the same period-dependent source model mentioned above. However, the M 8 class earthquakes such as the 1978 Mw 7.8 Miyagi-oki earthquake and the 2003 Mw 8.3 Tokachi-oki earthquake seem to have different characteristics, showing that the strong motion generation areas locate inside large slip areas considered to be "asperity". Then, the asperity areas have two to four times larger than the strong motion areas.

Keywords: the 2011 Tohoku earthquake, subduction earthquake, strong ground motion, characterized source model, strong motion generation area, the empirical Green's function method

Field Survey for the Memorial Matters from the 1923 Great Kanto Earthquake in Western Kanagawa Prefecture, Japan

TAKEMURA, Masayuki^{1*}

¹Disaster Mitigation Research Center, Nogoya-Univ.

Many memorial towers and monuments have been constructed for the heavy toll of life and for the restoration of villages or cities in Southern Kanto district. Death claimed a toll of about 105000 totally from the 1923 Great Kanto earthquake. These towers and monuments must be forever witnesses to the tragedy of the earthquake damage and spokesmen for the victim's dying wish "don't repeat such damages". However, most of them have been already forgotten by the citizens. We thought it's sacrilege and must use them for the public education of earthquake disaster prevention. This manuscript is a report on the field survey for the memorial matters from the Great Kanto earthquake in Western Kanagawa Prefecture and Atami, Ito Cites. The number of the matters is 170. This survey will be continued to the next year in Eastern Kanagawa Prefecture. The survey in Central Kanagawa Prefecture had been summarized in the last year.

Keywords: Great Kanto Earthquake, Memorial tower, Kanagawa Prefecture

Wave features Theory and Liquefaction

NISHIZAWA, Masaru^{1*}

¹none

Large liquefaction have an effect on many many house and building.

Conclusion

- (1) Large-scale liquefaction, the building is greatly influenced relation because of a phase shift.
- (2) The main point of liquefaction, look carefully wave features of principal shock.
- (3) In case of large-case liquefaction, wave mechanics theory is necessary.

Keywords: Wave Features Theory, Liquefaction, Phase, Relation

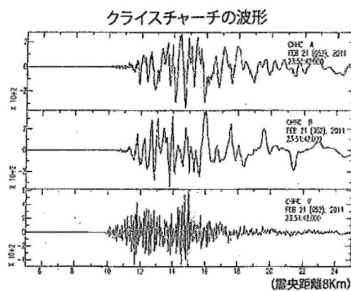


図-1

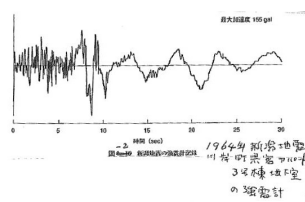


図-2

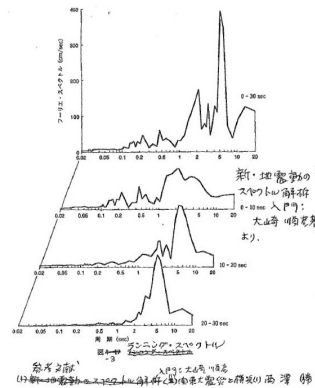


図-3

An additional correction term of ground-motion prediction equation for intra-plate earthquakes

MORIKAWA, Nobuyuki^{1*} ; FUJIWARA, Hiroyuki¹

¹NIED

Intra-slab earthquakes, which occur in a subducted ocean plate, radiates short-period seismic waves strongly compared with an inter-plate earthquakes with the same magnitude. It is pointed out that the strength of short-period seismic waves depends on the focal depth of the earthquake or has a difference by the plate. On the other hand, it is also pointed out that the radiation of short-period seismic waves from an outer-rise earthquake is as strong as that from an intra-slab earthquake whose focal depth is deep.

These things mean that it is important to model radiation characteristic of short-period seismic waves appropriately in the prediction of strong ground motions for intra-plate earthquakes. We propose a new ground-motion prediction equation (GMPE), but focal depth and/or plate dependence of the ground motion intensities are not considered. So we analyze strong ground motion records to investigate a new additional correction term of our GMPE for intra-plate earthquakes.

First we calculate the difference between observed amplitude and predicted one by using our GMPE for each records. And then we obtain "the source value" by averaging the difference for each earthquake and "the site value" by averaging the difference for each observation site. We examine the relation between "the source value" and the focal depth or difference in plates.

The "source value" of an intra-plate earthquake in the Pacific plate is large compared with an earthquake in the Philippine Sea plate. In addition, "the source value" becomes larger so that the focal depth becomes deeper. However, it is difficult to distinguish the effects of focal depth and/or different plates, because focal depths of intra-plate earthquakes in the Pacific plate are deeper than those in Philippine Sea plate in general. Therefore we think that it is better to model only one of these as the additional correction term of our GMPE.

Keywords: intra-slab earthquakes, outer-rise earthquakes, ground-motion prediction equation

Attenuation characteristics of strong ground motions in Chugoku, Shikoku and Kyushu districts

IKEURA, Tomonori^{1*}

¹Kajima Tech. Res. Inst.

I investigated attenuation characteristics of strong motions using data of K-NET and KiK-net in the southwest Japan. First, I evaluated relative site factors of 630 sites of K-NET and KiK-net in the area using adjacent sites network method[Ikeura and Kato,2011]. Secondly I converted spectra observed at those sites during large earthquakes to ones of base rock motions by cancelling site amplification effect using the relative site factor of each site. The converted high frequency amplitudes from the 2000 Western Tottori earthquake clearly show linear attenuation curves in the distance range of 10 to 500km. The converted amplitudes of the 2001 Geiyo earthquake, which occurred at the depth of 46 km in Philippine sea plate, also shows almost linear distribution in the distance range of 50 to 400km. In contrast with these events, the converted amplitudes of the 2014 Iyonada earthquake, which occurred at the depth of 78 km in Philippine sea plate, showed widely dispersed distribution, indicating complex attenuation characteristics due to tectonic setting beneath these area. Lower limit of the wide distribution is characterized by western sites beyond volcanic zone in Kyushu district, while upper limit is characterized by eastern sites in the fore arc area of Chugoku district and in Shikoku district.

Keywords: strong motions, attenuation characteristics, site factor, southwest Japan

Study on frequency and hypocentral distance dependent radiation coefficient

NAGASAKA, Yosuke^{1*}; NOZU, Atsushi¹

¹Port and Airport Research Institute

Modeling radiation coefficient is important because radiation coefficient transits from theoretical to average value at the frequency range that is important for structures.

We have investigated the records of the 2000 Western Tottori Earthquake and modeled frequency and hypocentral distance dependent radiation coefficient. We modeled the radiation coefficient as a weighted average of the theoretical and average radiation coefficient and the weighting coefficient is modeled so that it depends on frequency and hypocentral distance. We propose a weighting coefficient α expressed as $\alpha = \exp(-\pi f r / Q_R V_S)$. This means that the radiation coefficient approaches to the average value as the number of waves between the hypocenter and a station increases. Q_R is a coefficient that determines the dependence on frequency and hypocentral distance.

In this study, we apply the model to smaller earthquakes in order to eliminate the effect of complex source process that prevents from setting one theoretical radiation coefficient for each station.

Keywords: radiation coefficient, strong ground motion simulation

Effects of Accretionary Prisms on Long-Period Ground Motions Associated with Velocity Structure Models and Sources

GUO, Yujia^{1*}; KOKETSU, Kazuki¹; MIYAKE, Hiroe¹

¹Earthquake Research Institute, University of Tokyo

Subduction earthquakes along the Nankai Trough can generate significant long-period ground motions in the Osaka, Nobi, and Kanto basins. Accretionary prisms along the Nankai Trough play an important role to excite and prolong long-period ground motions. Yamada and Iwata (2005), Yoshimura *et al.* (2008), and Watanabe *et al.* (2014) reported that accretionary prisms can reduce amplitudes of direct waves and prolong durations of later phases. Goto and Nagano (2013) and Watanabe and Kato (2013) implied that the source location can control accretionary prism effects. Three-dimensional velocity structure models have been constructed for ground motion simulations in Japan. However, these models contain a larger uncertainty at the ocean region rather than the land region. There are only a few studies to validate S-wave velocity structure models, which affect seismic waves significantly. To evaluate precisely accretionary prism effects on long-period ground motions, we should take into account not only the uncertainty of velocity structure models but also the source diversity of subduction earthquakes. Furthermore, it is important to discuss accretionary prism effects in different frequency ranges, since long-period ground motions with different dominant periods are excited in the Osaka, Nobi, and Kanto basins.

We here performed three-dimensional simulations of long-period ground motions for the event (M_w 7.2) that occurred off the Kii peninsula at 10:07 on 5 September 2004 (UT), to clarify the variation of accretionary prism effects resulting from different accretionary prism models. Our simulations used three kinds of velocity structure models that are composed of a different accretionary prism model: (A) the Japan Integrated Velocity Structure Model (Koketsu *et al.*, 2008, 2012); (B) the model where the accretionary prism layer in the Model A is replaced with accretionary prism layers presented by the previous studies as Takahashi *et al.* (2002), Fujiwara *et al.* (2009, 2012), and Tsuji *et al.* (2011, 2014); (C) the model without accretionary prisms by replacing the S-wave velocity with 3.2 km/s. Long-period ground motions simulated for these models were compared in several frequency ranges. A finite element method with voxel meshes (Ikegami *et al.*, 2008) was used for simulations, and topography, ocean water as well as an attenuation with constant Q-value were implemented into the code. The valid frequency range was 0.05-0.3 Hz. We assumed the point source of Yamada and Iwata (2005) and used the source time function of Yagi (2004).

We then focused on the dependence of accretionary prism effects on seismic source as pointed out by previous studies, and investigated the performance of accretionary prism effects in terms of source location and rupture propagation effect using the above method and velocity structure models. We assumed several finite source models estimated by the Cabinet Office of Japan (2012).

Our simulations suggested that amplitudes of direct waves are not always smaller than those for the model without accretionary prisms, which is not consistent with the previous studies. In the Osaka and Nobi basins, the amplitude of peak ground motions at sites where sedimentary layers are thick is sensitive to the change of accretionary prism models. On the other hand, in the Kanto basin, such sensitivity is not significant and peak ground motions are attenuated because the main arrivals to the Kanto basin propagate through the accretionary prisms. We confirmed a difference in propagation characteristics at the eastern edge of the accretionary prisms between the Models A and B: for the Model B, later phases with periods of 9-12 sec at the Izu peninsula and the Kanto basin have a potential to be developed. We also indicated that the amplification effect of accretionary prisms on later phases is enhanced in the forward direction of rupture propagation for shallow sources located near the trough axis.

Keywords: Long-period ground motion, Accretionary prism, Nankai Trough, Subduction earthquake, Ground motion simulation, Velocity structure model

Long-period ground-motion observations and simulations in the Nankai Trough, southwest Japan

NAKAMURA, Takeshi^{1*} ; TAKENAKA, Hiroshi² ; OKAMOTO, Taro³ ; OHORI, Michihiro⁴ ; TSUBOI, Seiji¹

¹Japan Agency for Marine-Earth Science and Technology, ²Okayama University, ³Tokyo Institute of Technology, ⁴University of Fukui

We deployed a dense-array seafloor seismic observatory in the source area of great subduction earthquakes in southwest Japan in 2010. We observed the development of long-period motions in the seafloor strong-motion data at a moderate inland event (Mw 5.8) occurred in April 2013. The observed seismic waveforms are significantly prolonged and amplified, which does not agree with an empirical relation of amplifications for epicentral distances. We reproduce these features of waveforms at the seafloor stations in the period range of 10-20 s with FDM simulations and demonstrate the significant effects of seawater and sediment structures in ocean area on seismic wavefields. The long-period motions are predominantly caused by the propagation of surface waves developed within sediment layers in the subduction area. For the motions of the vertical component, the presence of a seawater layer also contributes to the developments. The snapshots in the cross section in depth show more trapped seismic energies and slower seismic-wave propagation in the subduction area than those in the land area, which produces the amplified and prolonged long-period motions at the seafloor stations. The snapshots in the horizontal plane show the distortion of concentric wave trains propagating from the source, indicating significant lateral variations of seismic velocity structures between land and ocean areas. The long-period range we analyzed is very important for magnitude estimations and moment tensor and finite-source analyses at great subduction earthquakes. Our observation and simulation results highlight the importance of ocean-specific structures for the seismic wave propagation and would contribute to advancing the seismic source studies and the strong-motion prediction by using seafloor station data.

Keywords: Long-period ground motion, strong motion, Nankai Trough, seafloor observation, DONET

Approach to broaden the period-range of long-period ground motion evaluation based on theoretical method

MAEDA, Takahiro^{1*}; IWAKI, Asako¹; MORIKAWA, Nobuyuki¹; IMAI, Ryuta²; AOI, Shin¹; FUJIWARA, Hiroyuki¹

¹NIED, ²Mizuho Information & Research Institute, Inc.

We have simulated long-period ground motions generated by megathrust earthquakes using various source models and 3D velocity structure model by the 3D finite difference method. To consider the influence of simulated ground motions on buildings, the analyzing period range of our simulation (3 - 20 seconds) was too long for most buildings. In this study, we examine the effects of more detailed velocity structure and seismic source models to broaden the analyzing period range.

As for the structure model, we used a newly constructing subsurface structure model (Senna et al., 2013, JDR) for the southern Kanto area. This model includes not only a deeper structure model but shallower layers than the engineering bed rock. By constructing deep and shallow structure model simultaneously, it is expected to improve ground motion simulation for period from 0.5 to 2 seconds. We assume two velocity structure models; one has shallow structure ($V_s=250\text{m/s}$) as a surficial layer (SD model) and other includes only the deep structure model (surficial layer has V_s of 500m/s) (D model). By comparing the simulated results assuming a point source, peak amplitude and duration for SD model are larger than those of D model. Simulated Fourier spectra indicated that the difference of two models is dominant at period shorter than about 2 second.

As for the source model, we used a characterized source model and uniform rupture velocity was assumed. In this study, we introduce a multi-scale heterogeneity (Sekiguchi and Yoshimi, 2006) to rupture propagation. We construct 274 source models for the Sagami Trough megathrust earthquake assuming different source area, hypocenter and asperity configuration and put the rupture heterogeneity on these source models. Influence of the rupture heterogeneity seems larger for shorter period range and is vary with hypocenter and asperity configuration.

To broaden a valid period range of long-period ground motion simulation, the shallow slower velocity layers and multi-scale heterogeneity of source model are worth taking it consideration. In addition, considering the appropriate simulation method is important, especially for long-period ground motion simulation, which needs a long-duration calculation.

This study was supported by the Support Program for Long-Period Ground Motion Hazard Maps by the Ministry of Education, Culture, Sports, Science and Technology (MEXT).

Keywords: long-period ground motion, FDM, velocity structure model, multi-scale heterogeneity

Broadband ground motion simulation techniques applied to megathrust earthquakes in the Sagami trough

IWAKI, Asako^{1*} ; MAEDA, Takahiro¹ ; MORIKAWA, Nobuyuki¹ ; FUJIWARA, Hiroyuki¹

¹NIED

Long-period (~1s and longer) ground motion are generally evaluated by a theoretical computation method based on appropriate models of rupture process and three-dimensional (3D) wave propagation process. We have been working on seismic hazard assessment for long-period ground motion of various scenarios of the megathrust earthquakes in the Sagami trough (e.g. Iwaki et al. 2014, JEES). The period range of the analysis was limited to 3s and longer due to the resolution of the source and velocity structure models.

On the other hand, it is necessary to include shorter-period ground motion to the seismic evaluation as the source fault on the Sagami trough lies directly beneath the metropolitan area. In order to achieve this goal, Maeda et al. (2015, this meeting) apply short-scale source and velocity structure models in the ground motion simulation by theoretical computation method. This paper presents alternative approach: broadband ground motion simulation techniques that include stochastic or semi-empirical methods.

We apply the “hybrid method” for broadband ground motion simulation by NIED (e.g. Senna et al. 2004) to M8 class earthquakes in the Sagami trough. It is the hybrid of finite-difference method (FDM) and the stochastic Green’s function (SGF) method in the long- and short-period ranges, respectively. In addition, we try another method proposed by Iwaki and Fujiwara (2013) and compare the methods. The latter method simulate high-frequency (short-period) ground motion using low-frequency (long-period) ground motion and the empirical “envelope ratio function (ERF)” between high- and low-frequency acceleration envelopes.

For both methods, the long-period ground motion is computed by a 3D FDM (GMS; Aoi et al., 2004) and combined with the short-period ground motion at the cross-over period 2s.

We compared the methods in terms of the computed velocity waveforms and Fourier spectra at several sites within the Kanto plain. The amplitude levels of the main motion for the two methods are similar to each other. However, the considerable difference is observed at some sites in the later phases where hybrid method produces smaller short-period components.

In order to compare and investigate the appropriateness of the two methods, it is necessary to compare the resulting ground motion with the GMPEs. We aim to utilize these methods in broadband seismic hazard evaluation.

Keywords: megathrust earthquake, long-period ground motion, broadband ground motion, Sagami trough, Kanto plain

Simulation of irregular wave generation due to fault formation by an elasto-plastic finite deformation analysis

YAMADA, Shotaro^{1*} ; NODA, Toshihiro¹ ; ASAOKA, Akira²

¹Nagoya University, ²Association for the Development of Earthquake Prediction

The authors, in the past study¹⁾, simulated shear bands formation in ground due to strike-slip fault by using a soil-water coupled finite deformation code taking into inertia force, **GEOASIA**²⁾. In the present study, the analysis code was employed to simulate formation of normal and reverse faults and wave generation due to the formation assuming a ground composed of a highly brittle soil. The analysis code mounts the SYS Cam-clay model³⁾ as an elasto-plastic constitutive model which can describe a wide variety of soils within the same theoretical framework. Also, since the rate-type equation of motion is precisely time-integrated, progressive failure will be analyzed as a nonlinear dynamic problem, and then generation and/or propagation of waves induced by shear bands formation will also naturally be developed in the analysis^{4),5)}. Making use of this characteristic, wave generation induced by fault formation was focused on. When the ground was compressed from lateral faces by displacement control under plane strain condition, a reverse fault-like failure was generated as a progressive failure with strain localization (Figure 1). At that time, elastic energy accumulated on the non-destructive area at the compression stage was released at once. In the case of a horizontally stratified ground, as failure progresses rapidly, acceleration motion was reached to the max. at first motion and decayed exponentially with time in a similar way that artificial earthquake shows (Figure 2). On the other hand, in the case of a ground with initial random imperfections, as some small failure events exist in a large failure event, an irregular wave like a natural seismic wave was generated (Figure 3). On the other hand, when the ground with the initial random imperfections was extended from lateral side by strain control, a normal fault was generated and another irregular wave was generated.

1) Noda, T., Yamada, S., Asaoka, A. and Kawai, Y. (2014): Numerical simulation of shear bands formation in ground due to strike-slip fault, *Japan Geoscience Union Meeting 2014*, SSS31-08.

2) Noda, T., Asaoka, A. and Nakano, M. (2008): Soil-water coupled finite deformation analysis based on a rate-type equation of motion incorporating the SYS Cam-clay model, *Soils and Foundations*, **48(6)**, 771-790.

3) Asaoka, A., Noda, T., Yamada, E., Kaneda, K. and Nakano, M. (2002): An elasto-plastic description of two distinct volume change mechanisms of soils, *Soils and Foundations*, **42(5)**, 47-57.

4) Noda, T., Xu, B. and Asaoka, A. (2013): Acceleration generation due to strain localization of saturated clay specimen based on dynamic soil-water coupled finite deformation analysis, *Soils and Foundations*, **53(5)**, 653-670.

5) Asaoka, A., Yamada, S. and Noda, T. (2013): Numerical analysis of failure of soil ground due to surface loading and generation of vibration induced by the failure, *Japan Geoscience Union Meeting 2013*, SSS28-18.

Keywords: natural fault, reverse fault, seismic wave, strain localization, inertial force, elasto-plastic body

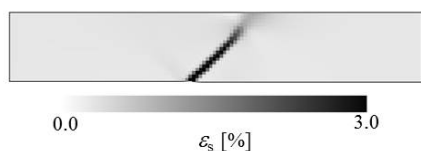


Figure 1. Reverse fault-like failure (shear strain distribution)

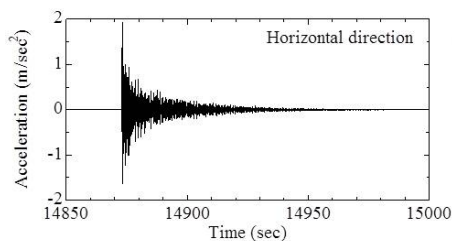


Figure 2. Wave generated in a horizontally stratified ground

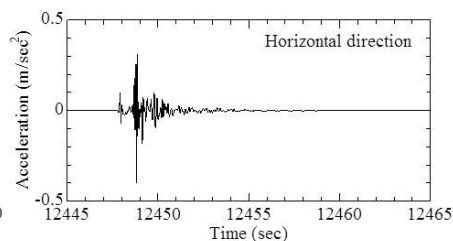


Figure 3. Wave generated in a ground with initial random imperfections

Estimation of shallow shear wave velocity in Bandung basin, Indonesia using horizontal to vertical (H/V) spectral ratio

PRAMATADIE, Andi muhamad^{1*} ; CHIMOTO, Kosuke¹ ; AFNIMAR, Afnimar² ; YAMANAKA, Hiroaki¹

¹Tokyo Institute of Technology, ²Bandung Institute of Technology

Bandung, the third populous city in Indonesia with population of around 2.7 million, is located in the western part of Java island. The city lies on a basin structure called Bandung basin. The concern of seismic risk in this area becomes important as existing of 24 km-long Lembang fault in the northern part. As part of potential seismic hazard estimation, Microtremors measurement is one of effective tool to estimate shear wave velocity profile and site amplification factor, especially in the urban area. A 3 component microtremors measurement is conducted in 76 sites to observe horizontal-to-vertical (H/V) spectral ratio that reflected to the ground characteristic. In the previous work, the obtained shear wave velocity models from Spatial Autocorrelation (SPAC) are used as reference model. Estimation of the ground structures are using the tuning factor to fitting the observed H/V spectrum with the theoretical ellipticity of fundamental mode of Rayleigh wave from the velocity model. From the obtained velocity model, we observed the thicknesses of soft layer (<500 m/s) from north to south of basin are changing from around 8 to 12 m in edge of basin area and around 40 m at the central of basin. The obtain profiles provide detail structure information in Bandung basin. Also the calculation of AVS30s and site amplification factor were conducted in each site, to understand the potential seismic hazard in the area. We also discuss a spatial variation of the amplification of earthquake ground motion using the obtained profiles.

Keywords: H/V spectral ratio, S-wave velocity, shallow soil, Bandung basin, amplification

An evaluation to trace phase of surface wave using the seismic interferometry

MOTOKI, Kentaro^{1*} ; KATO, Kenichi¹

¹Kobori Research Complex

Using seismic interferometry, group velocities between 2 sites have been successfully evaluated from microtremor long term records by previous researches. If seismic interferometry can reproduce Green's function, we can estimate not only group velocities but also phase traces. In this study, we propose a method to evaluate propagation of surface waves, confirm the validity through the numerical test, and show application to the observed data.

We calculate deconvolution waveform against cross correlation at the end of the target area, in order to trace the propagation of surface waves on the target area. In numerical test, the waves from the surrounding sources were calculated using the reciprocity theory to represent the equipartition wave field. We set subsurface structure the 2 layer models, which are stratified model, 2 dimensional irregular model and 3-dimensional irregular model. The Green's function, which was regarded as a correct result, was calculated by the point force with FDM, and we confirmed the validity of the result of seismic interferometry.

The result of seismic interferometry of the stratified model corresponds to the result of Green's function. With the 2 dimensional and 3 dimensional irregular models, the result of the seismic interferometry successfully reproduced the Green's function only for the propagation from the rock area to the sedimentary area, and it is necessary to pay an attention about the direction in calculation of deconvolution and seismic interferometry.

We apply this method to Hi-net stations whose codes are N.ICWH and N.ICEH. The results using 2 reference sites are consistent each other and correspond to the results using 3 dimensional subsurface model.

For future works, we will apply this method near the edge of the Kanto basin to trace the generation of the surface wave induced by basin edge.

Keywords: seismic interferometry, deconvolution